ASTROMETRY WITH LSST: OBJECTIVES AND CHALLENGES

D. I. Casetti-Dinescu,[1,2] T. M. Girard,[2] R. A. Méndez,[3] and R. M. Petronchak[1]

RESUMEN

El venidero Large Synoptic Survey Telescope (LSST) es un telescopio óptico con una apertura efectiva de 6.4 m, y un campo de visión de 9.6 grados cuadrados. Por tanto, el LSST tendrá un étendue más grande que cualquier otro telescopio óptico, pudiendo tomar imágenes profundas y de amplio campo del cielo. Hay cuatro amplias categorías entre sus objetivos científicos: 1) materia y energía oscuras, 2) eventos transitorios, 3) Vía Láctea y sus vecinos y, 4) Sistema Solar. En particular, para el caso científico de la Vía Láctea, la astrometría hará una contribución crítica; por lo tanto debe prestarse especial atención para extraer la mayor cantidad de información astrométrica de los datos del LSST. Acá describimos someramente los retos astrométricos impuestos por tan masivo sondeo. También presentamos algunos ejemplos actuales de cámaras de campo ancho profundas ubicadas en la superficie terrestre usadas para astrometría, como precursores del LSST.

ABSTRACT

The forthcoming Large Synoptic Survey Telescope (LSST) is an optical telescope with an effective aperture of 6.4 m, and a field of view of 9.6 square degrees. Thus, LSST will have an étendue larger than any other optical telescope, performing wide-field, deep imaging of the sky. There are four broad categories of science objectives: 1) dark-energy and dark matter, 2) transients, 3) the Milky Way and its neighbours and, 4) the Solar System. In particular, for the Milky-Way science case, astrometry will make a critical contribution; therefore, special attention must be devoted to extract the maximum amount of astrometric information from the LSST data. Here, we outline the astrometric challenges posed by such a massive survey. We also present some current examples of ground-based, wide-field, deep imagers used for astrometry, as precursors of the LSST.

Key Words: astrometry — proper motions

1. INTRODUCTION

The LSST is an optical and near-IR telescope that will survey half of the sky in six filters (ugrizy) down to $r \sim 27.5$ (for co-adds), with about 1000 visits over ten years. Each visit consists of 2×15 sec exposures, reaching $r \sim 24.5$ per visit. The telescope design represents a new concept meant to have the largest étendue to date (320 $m^2 deg^2$) with the purpose of achieving a wide-fast-deep survey to address a wide range of science topics. Construction began at Cerro Pachón, Chile in April 2015, and the system is planned to start full science operations in 2023. The LSST camera — the largest ever constructed — is the size of a small car weighing some 2800 kg, and it is designed to provide a 3.5-degree diameter field of view with 10 μm pixels, at $0''.2$ per pixel. The detector is a mosaic of 189 CCDs with a total of 3.2 Gigapixels, collecting some 15 Terabytes of data per night. The survey is expected to produce some 40 billion objects, half being stars and the other half galaxies[4].

In this contribution, we focus on one of the four LSST science themes, namely the study of the Milky Way (MW) and its neighbours via resolved stellar populations. The survey will re-address the accretion history of the MW by probing the far reaches of our Galaxy: main sequence stars out to 100 kpc, and RR Lyrae stars out to 400 kpc (compared to 10 kpc for *Gaia* and SDSS, for the former stars, and 100 kpc for SDSS and RR Lyrae stars). In the Solar neighbourhood, LSST will provide a census of all stars and their fundamental properties within 300 pc of the Sun. Unlike previous large photometric surveys, LSST is dedicated to obtaining high-quality astrometry — meaning parallaxes and proper motions — adequate for addressing various science objectives. In this sense, besides the Science Collaborations, there is an active Differential Astrometry Group[5] that is active along these goals.

[1]Physics Department, Southern Connecticut State University, New Haven, CT, USA (dana.casetti@gmail.edu).

[2]Yale Southern Observatory, P.O. Box 208101, New Haven, CT, USA (terrence.girard@gmail.com).

[3]Departamento de Astronomia, Universidad de Chile, Casilla 36-D, Santiago, Chile (rmendez@uchile.cl)

[4]http://www.lsst.org

[5]https://listserv.lsstcorp.org/mailman/listinfo/lsst-dawg

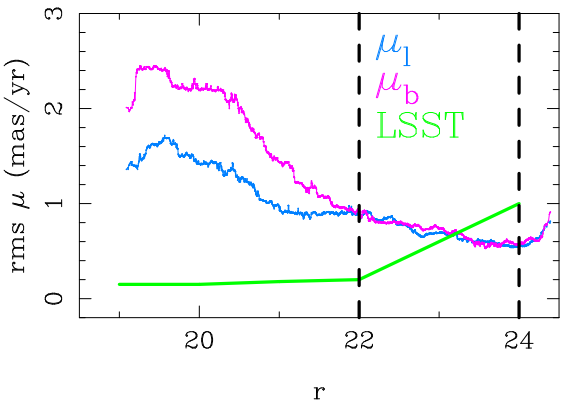

Fig. 1. RMS proper motion of blue ($(r-i) < 0.4$) field stars as a function of r magnitude, in the direction $(l, b) = (86°, 35°)$ (Besancon model). Compare with the LSST proper-motion error prediction (Ivezić, Beers & Jurić 2012). The vertical dashed lines indicate the magnitude of old main-sequence turnoff stars at 40 kpc and at 100 kpc.

2. EXPECTED ERRORS

Each of the 189 CCDs of the mosaic detector is made of 16 segments with individual readout. Each segment is 500×200 pix, at $0\farcs2$/pix, such that one CCD is about $13.6'$ on a side. The CCDs are arranged in 3×3 rafts with some $41'$ on a side. The estimated positional precision for a well-measured star is 10 mas over a radius of $20'$. Projected proper-motion errors and parallax errors are derived from this nominal number as a function of S/N, repeats and time baselines (see LSST Science Collaborations white paper on Observing Strategy, 2016, Ivezić, Beers & Jurić 2012). In Figure 1, we show the rms proper motion of blue field stars as a function of magnitude as predicted by the Besancon model (Robin et al. 2003). The proper-motion error curve from Ivezić, Beers & Jurić (2012) is also shown, together with marks of the magnitude of old turnoff stars at 40 and at 100 kpc. Cleary, predicted proper-motion errors are smaller than the proper-motion dispersion of the field down to $r \sim 23$, thus enabling an easy detection of kinematically cold tidal streams in the outer halo via proper motions only.

Predicted parallax errors are 0.6 mas at $r = 21$ to about 3 mas at $r = 24$; however a more detailed characterisation, within the framework of the "Basic Cadence," can be found in the LSST Science Collaborations white paper on Observing Strategy, (2016). These error levels will enable the detection of $\sim 10^5$ M dwarfs within 300 pc, thousands of L/T brown dwarfs within tens of pc, and the white dwarf luminosity function for the thin and thick disks, and halo.

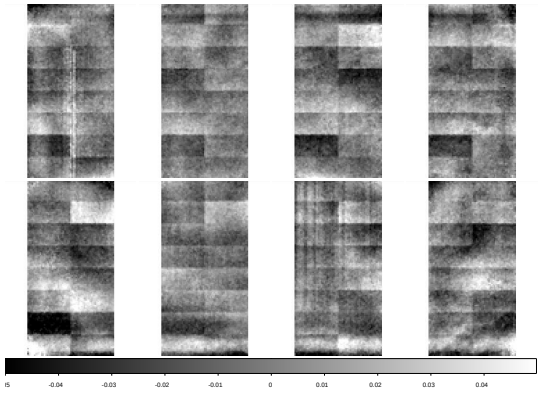

Fig. 2. Map of Y (Dec.) residuals for each WFI chip ($8' \times 16'$). The rectangular boxlike pattern has an amplitude of ~ 0.02 pix (5 mas). Residuals in each 2K x 4K chip are binned and averaged in cells of 32x32 pixels. Typically, there are some 40 measurements per cell.

3. CHALLENGES

3.1. *Lithographic and/or Other Causes of Patterns in CCDs: The WFI Example*

Large-scale distortions over the field-of-view are generated by the optical assembly, and are usually modelled with polynomials. Here, we focus on small-scale distortions, of specific pattern, which are owed to the CCD chip itself. These appear as a result of the spatial irregularities in the pixel grid, such as a lithographic pattern seen in the *HST* Wide Field Camera 3 (Kozhurina-Platais et al. 2016), or as a result of electric fields transverse to the surface of the CCD that generate "tree ring" patterns and "edge distortions" in thick, back-illuminated, fully-depleted CCDs such as those employed by the Dark Energy Survey or the LSST (Plazas, Bernstein, & Sheldon 2014). Amplitudes of these effects are 0.1 pixels (4 mas) in the former example and 0.056 pix (15 mas) in the latter example.

Here we present another example, that of the Wide Field Imager (WFI) on the 2.2 m ESO telescope. The WFI is a 2K x 4K 8-chip mosaic detector.

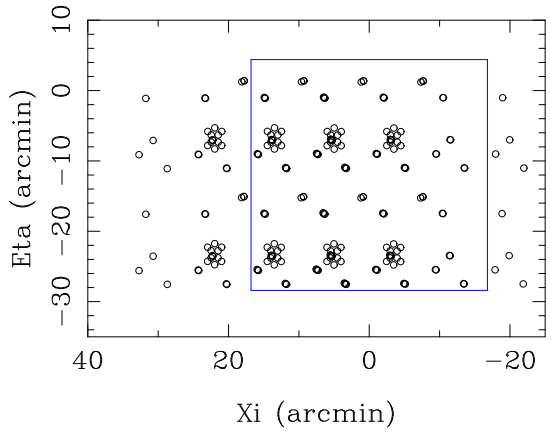

Fig. 3. Offsets of the 29 exposures in the Plaut window, for each WFI chip. The box frame shows the approximate area of the entire WFI. The field center is at $(l, b) = (274.5°, -32.9°)$. Note the various sizes of the offsets, chosen to map both large- and small-scale distortions.

Data were collected in the Bulge's "Plaut window," in 2012. A total of 29 40-sec, V-band exposures of various offsets and dithers were used to build the residual mask shown in Figure 2. The mask was obtained after individual exposures were transformed into an average catalog (using up to 4-th order polynomials). The amplitude of the pattern is ~ 0.02 pixels (5 mas). Previous astrometric studies with this WFI (Anderson et al. 2006, Bellini et al 2009) did not capture this pattern because of insufficient mapping of the detector: see in Figure 3 the offset pattern employed in our study.

3.2. *Astrometry of Galaxies versus Stars*

Background galaxies are used to define the inertial reference frame, or zero point of the absolute proper-motion system. It is thus fundamental that galaxies and stars behave similarly in astrometric analyses. Often times, it is not the centering precision (and algorithm) that is critical, but rather being able to place stars and galaxies on a similar system. For instance, charge transfer efficiency (CTE) may affect differently the images of galaxies versus stars (e.g., Casetti-Dinescu & Girard 2016). Some ways to tackle this problem are 1) to choose round, centrally concentrated galaxies that have PSF's similar to those of stars (see *HST*-related work), 2) monitor galaxies and stars in a wide magnitude range and model their behaviour, and/or 3) use stars from an astrometric catalog such as *HIPPARCOS* or *Gaia* instead of galaxies for proper-motion reference.

3.3. *Gaia as a Proper-motion Reference System*

The potential of *Gaia* as a calibrating tool for deep, ground-based surveys is tremendous. Here we outline some of the caveats relative to LSST. The LSST survey's saturation limit is at $r \sim 16$ with the useful bright end at $r \sim 20$ where CTE effects may be strong, while *Gaia*'s faint end is at $r \sim 20 - 21$, where proper-motion errors are of the order of 0.3 mas/yr, comparable or larger than LSST predicted errors. Thus the magnitude overlap between LSST and *Gaia* is at a non-optimal region of each survey. Finally, LSST's 4K x 4K CCD sensors are some $13.6'$ on a side (leaving aside that each is formed from 16 segments). Within this $13.6' \times 13.6'$ area, one expects of the order of 1300 stars to $r < 21$ in regions toward the Galactic center; however at the South Galactic Pole, only some 80 stars are expected. Thus, in some regions, relying solely on *Gaia* calibration might be insufficient. Nevertheless, combining internal LSST calibrations (such as that described here for the WFI) together with *Gaia* calibrations can assure a robust astrometric methodology to best exploit a survey such as the LSST.

REFERENCES

Anderson, J., Bedin, L. R., Piotto, G. Yadav, R. S., & Bellini, A. 2006, A&A454, 1029

Bellini, A., Piotto, G., Bedin, L. R., Anderson, J., Platais, I., Momany, Y., Moretti, A., Milone, A. P., & Ortolani, S. 2009, A&A493, 959

Casetti-Dinescu, D. I. & Girard, T. M. 2016, MNRAS 461, 271

Ivezić, Z., Beers, T. C. & Jurić, M. 2012, ARAA 50, 521

Kozhurina-Platais, V., Mackenty, J., Golimovsky, D., Sirianni, M., Borncamp, D., Anderson, J., & Gorgin, N. 2016, in Proceedings of SPIE, Vol. 9904, p. 6

LSST Colab. 2016, https://github.com/LSSTScienceCollaborations/ObservingStrategy

Plazas, A. A., Bernstein, G. M., & Sheldon, E. S. 2014, PASP, 126, 750

Robin, A. C., Reylé, C., Derrière, S. & Picaud, S. 2003, A&A409, 523